# Tactile and Bone-conduction Auditory Brain Computer Interface for Vision and Hearing Impaired Users - Stimulus Pattern and BCI Accuracy Improvement

Hiromu Mori*, Shoji Makino*,† and Tomasz M. Rutkowski*,†,▽
*TARA Life Science Center, University of Tsukuba, Tsukuba, Japan
†RIKEN Brain Science Institute, Wako-shi, Japan
E-mail: tomek@bci-lab.info (▽corresponding author)
Website: http://bci-lab.info/

***Abstract*—This paper aims to improve tactile and bone–conduction brain computer interface (tbaBCI) classification accuracy based on a new stimulus pattern search in order to trigger more separable $P300$ responses. We propose and investigate three approaches to stimulus spatial and frequency content modification. As result of the online tbaBCI classification accuracy tests with six subjects we conclude that frequency modification in the previously reported single vibrotactile exciter–based patterns leads to border of significance statistical improvements.**

## I. Introduction

The contemporary brain–computer interfaces (BCIs) are typically based on mental visual or motor imagery paradigms, which require extensive user training and good eyesight from the users [1]. Recently alternative solutions have been adopted successfully to make use of spatial auditory [2] or tactile (somatosensory) sensory modalities [3], [4], [5], [6], [7] to improve BCI usage comfort and to increase the information transfer rate (ITR) achieved by users. Two recent reports published by the authors in [8], [9] have shown combination of two above–mentioned modalities, which rely on $P300$ response evoked by the audio and tactile stimuli delivered simultaneously via vibrotactile exciters attached to the head positions, thus benefiting from the bone–conduction effect for audio. This offers a viable alternative for individuals lacking somatosensory afferent neural fibers transmission from peripheral body locations.

This paper reports improvement of our previously reported tbaBCI paradigm [8] based on suitable stimulus spatial patterns that subject can easily distinguish and as a result evoked stronger in amplitude in EEG the $P300$ responses. We propose to create stimulus patterns using multiple subsets of the vibrotactile exciters using also various stimulation frequencies. The above steps are meaning to give the user a clear spatial and frequency pattern based cues leading to simpler discrimination among the presented tactile and bone–conduction auditory stimuli.

The rest of the paper is organized as follows. The next section introduces the materials and methods used in the study. It also outlines the experiments conducted within the presented project. The results obtained in EEG online and offline experiments with six BCI subjects are then discussed. Finally, conclusions are formulated and directions for future research are outlined.

## II. Materials and Methods

Six volunteer male BCI subjects participated in the experiments. The subject's mean age was $25.83$, with a standard deviation of $8.17$. All the experiments were performed at the Life Science Center of TARA, University of Tsukuba, Japan. The psychophysical and online (real–time) EEG tbaBCI paradigm experiments were conducted in accordance with the *WMA Declaration of Helsinki Ethical Principles for Medical Research Involving Human Subjects.* The experimental procedures were reviewed by the Ethical Committee of the Faculty of Engineering, Information and Systems at University of Tsukuba, Tsukuba, Japan (experimental permission number $2013R7$).

### A. Tactile and Bone–conduction Auditory Stimulus

The tactile and bone–conduction auditory stimulus was created as a square acoustic frequency wave generated by the ARDUINO micro–controller board with a custom built battery–driven and electrically isolated multichannel power amplifier. An in–house developed software managed the above device from *MAX/MSP* visual programming environment. The stimuli were delivered to the subject's head locations via the vibrotactile exciters HiWave HIAX19C01-8 operating in the acoustic frequencies of $300 \sim 20,000$ Hz, as depicted in Figure 1. The subject attended (button–press responded in case of psychophysical or mentally counted only in case of EEG experiments) only to the instructed *target* locations, while ignoring the other stimuli (we assigned labels to the attended stimulus as *target* and to the other ignored as *non–target*). The instructions were presented visually by means of the *MAX/MSP* program in psychophysical experiment and *BCI2000* program in EEG experiment.

978-616-361-823-8  

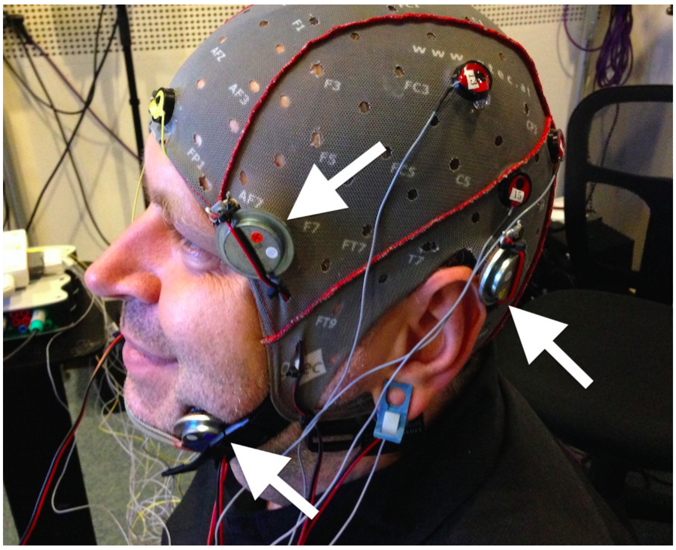

Fig. 1. User's head with EEG cap with embedded electrodes and vibrotactile exciters (indicated by the white arrows in the picture) attached. The photograph is reproduced with the user permission.

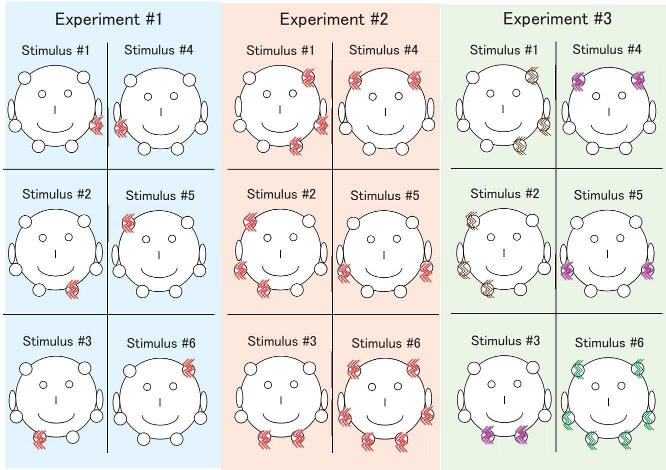


Fig. 2. The spatial setting for the tactile and bone–conduction auditory stimulus patterns used in the experiments reported in this paper. The circles drawn on face icons represent the vibratactile exciter locations. The color wavy lines depict the stimulus spatial configurations of the exciters used in each pattern. The line colors represent the stimulus frequencies (red 350 Hz; brown 300 Hz; purple 500 Hz; and green 700 Hz respectively).

In this study, we conducted three experiments to test the proposed new stimulus patterns' effectiveness. In each of the conducted experiments six different stimulus patterns were used. In the experiment #1 the stimuli were delivered to the user's head by single vibrotactile exciters as depicted in Figure 2. This setting was the same as in our previous studies [8], [9] in order to compare brainwave responses with the current setup of the tactile and bone–conduction auditory stimulus patterns introduced in this paper. In the experiment #2 the stimuli were composed of multiple vibrotactile exciters combined together. Each stimulus pattern in the experiment #2 has been also depicted in the middle column of Figure 2. Based on our previous studies [8], [9] and user reports we decided to stimulate larger head areas to avoid mistakes caused often by close spatial proximity of the vibrotactile exciters embedded within the EEG cap. In the both experiments #1 and #2 the same stimulus frequency of 350 Hz was used. Only in the experiment #3 we used various frequencies in order to add more discriminative features for the users (see also Figure 2 for details).

### *B. Psychophysical Experiment Protocol*

The psychophysical experiment was conducted to investigate the stimulus pattern possible influences on the subject's response time and accuracy. The behavioral responses were collected using a computer keyboard and the *MAX/MSP* program. Each subject was instructed which stimulus to attend by a red color circle shown on a computer display and generated by the instruction program as shown in Figure 3. The subject was instructed to press the response button (any key on a keyboard) with the dominant hand when the *target* stimulus was presented in a series of random distractors (as in a classical oddball paradigm [1]).

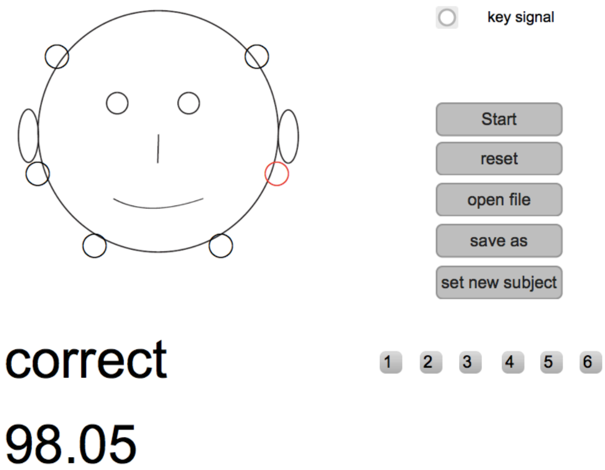


Fig. 3. The visual instruction screen presented to the subject during the psychophysical experiment created in the *MAX/MSP* environment. The circles represent vibrotactile exciters and the red color indicates the *target*.

Each trial was composed of 100 ms long tactile stimuli delivered in a randomized order to each head location separately with an inter–stimulus–interval (ISI) of 900 ms. Every random sequence thus contained a single *target* and five *non–targets*. A single run included 10 sequences (resulting in 60 *targets* and 300 *non–targets*). Details of the psychophysical experimental protocol are summarized in Table I.

### *C. EEG Experiment Protocol*

EEG signals were captured with an EEG amplifier system vAmp by Brain Products GmbH, Germany, using g.GAMMAbox with connected active electrodes *g.LADYbird* by g.tec Medical Instruments GmbH, Austria. The electrodes were attached to the head locations: *Cz, Pz, P3, P4, C3,*

TABLE I
THE PSYCHOPHYSICAL EXPERIMENT CONDITIONS

| Experimental condition | Detail |
|---|---|
| Number of subjects | 6 |
| Stimulus length | 100 ms |
| Vibrotactile frequencies | experiment #1 350 Hz<br>experiment #2 350 Hz<br>experiment #3 {300,500,700} Hz |
| Inter–stimulus–interval (ISI) | 900 ms |
| Tactile stimulus device | HiWave HIAX19C01-8 |
| Subject response input device | Computer keyboard |
| Number of sequences | 10 |
| Number of runs | 1 |

*C4, CP5, and CP6* as in the $10/10$ extended internatio system [10]. The ground electrode was attached to *FPz* ] sition and reference to the left earlobe respectively. No el tromagnetic interference was observed from the vibrotac exciters operating in higher frequencies comparing to the El frequency spectrum. Details of the EEG experimental protocol are summarized in Table II.

The recorded EEG signals were processed by the in–house extended *BCI2000* [11], [12], [13] using a stepwise linear discriminant analysis (SWLDA) classifier [14] with features drawn from the $0 \sim 800$ ms ERP latency intervals. The sampling rate was set at $500$ Hz, the high pass filter at $0.1$ Hz, and the low pass filter at $40$ Hz. The ISI was set to $400$ ms, and each stimulus duration was $100$ ms. The subjects were instructed which stimulus to attend by visual instruction presented on a computer screen using the same interface as in the psychophysical experiment presented in Figure 3. Each run included ten sequences (randomized $60$ *targets* and $300$ *non–targets* each), and the averages of ten ERPs were later used for the classification. Each subject performed three runs (resulting in $180$ *targets* and $900$ *non–targets*), which were later averaged as discussed in the next section.

## III. RESULTS

The results comparison the three setups tested in psychophysical and online BCI EEG experiments are summarized in the following sections.

TABLE II
THE EEG EXPERIMENT CONDITIONS

| Experimental condition | Detail |
|---|---|
| Number of subjects | 6 |
| Stimulation length | 100 ms |
| Vibrotactile frequency | experiment #1 350 Hz<br>experiment #2 350 Hz<br>experiment #3 $\{300, 500, 700\}$ Hz |
| Inter–stimulus–interval (ISI) | 400 ms |
| EEG recording system | vAamp and g.GAMMAbox with active EEG electrodes |
| Number of electrodes | 8 |
| EEG electrodes positions | *Cz, CPz, P3, P4, C3, C4, CP5, CP6* |
| Reference and ground electrodes | earlobe and *FPz* |
| Tactile stimulus device | HiWave HIAX19C01-8 |
| Number of sequences | 10 |
| Number of runs | 3 |

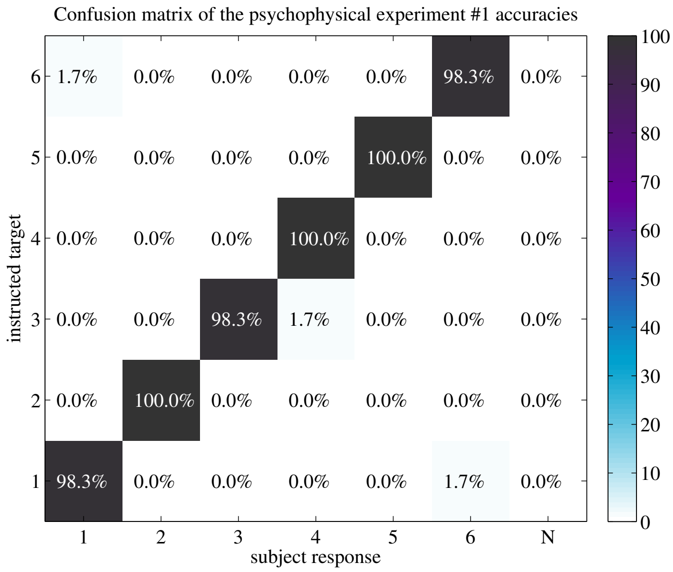


Fig. 4. Confusion matrix resulting from the psychophysical experiment #1 of all the six subjects in form of a grand mean average responses. The diagonal of the above matrix depicts the correct response rates, while the off–diagonals the mistakes. The last (seventh and marked with a letter $N$) column illustrates the lack of misses (no responses) in our experiment. The color–coding, summarized with the color–bar on the right of the plot, visualizes the response rates.

### A. Psychophysical Experiment Results

The psychophysical experiment accuracy results are depicted in form of a confusion matrices in Figures 4, 5, and 6. The confusion matrices with majority of accurate responses depicted on diagonals confirmed experimental designs validity and low difficulties for the tested participants. The boxplot psychophysical response time distributions are presented in Figures 7, 8, and 9. Each response time distribution results further confirmed the stimulus related cognitive load similarity since the behavioral responses for all the patterns were basically the same (as resulted with non–significant median differences from pairwise Wilcoxon–tests). This finding validated the design of the following tbaBCI EEG experiments.

### B. EEG Experiment Results

The grand mean averaged results of the conducted online BCI EEG experiments with the six participating subjects are presented in Figures 10, 11, and 12 in form of matrices depicting ERP latencies with $P300$ responses together with the area under the curve (AUC) feature separability analyses. We report also the averaged head topographic plots of the evoked responses at the highest and lowest ERP separability latencies in the *target versus non–target* averaging scenario as elucidated by AUC maxima and minima. The highest averaged differences were found at $398$ ms, $444$ ms and $392$ ms, which perfectly aligned the $P300$ response peaks in grand mean average ERP plots.

Figure 13 depicts time series of all electrodes with *target* and *non–target* responses from the three EEG experiments

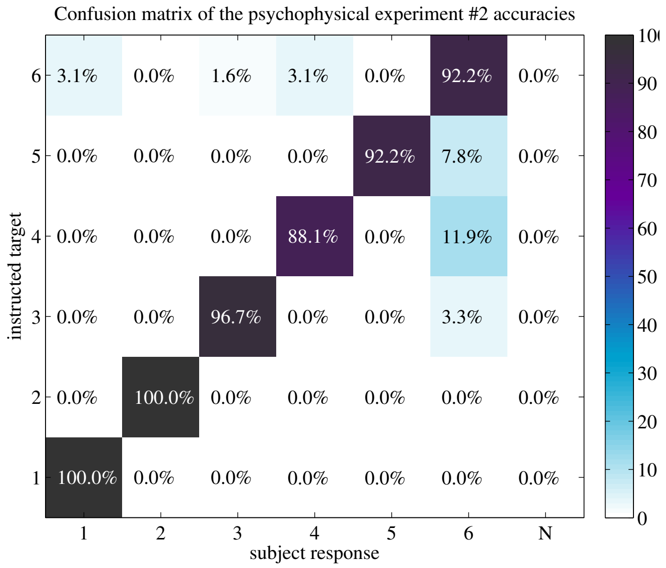


Fig. 5. Confusion matrix resulting from the psychophysical experiment # of all the six subjects in form of a grand mean average responses. Th diagonal of the above matrix depicts the correct response rates, while the off diagonals the mistakes. The last (seventh and marked with a letter $N$) column illustrates the lack of misses (no responses) in our experiment. The color–coding, summarized with the color–bar on the right of the plot, visualizes the response rates.

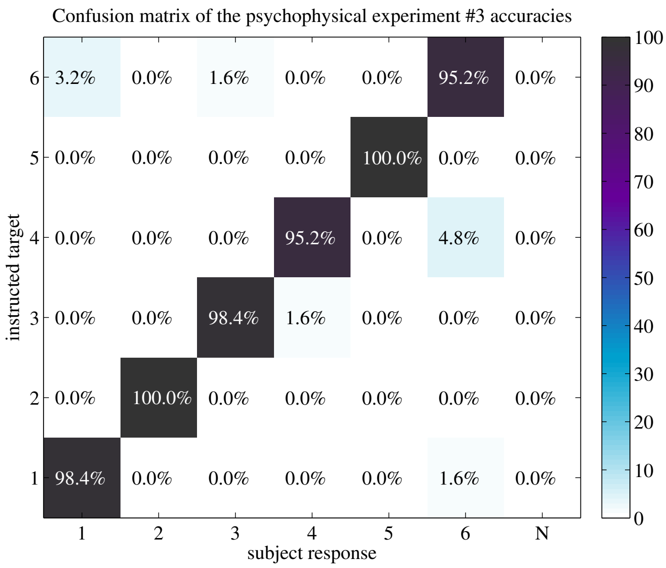


Fig. 6. Confusion matrix resulting from the psychophysical experiment #3 of all the six subjects in form of a grand mean average responses. The diagonal of the above matrix depicts the correct response rates, while the off–diagonals the mistakes. The last (seventh and marked with a letter $N$) column illustrates the lack of misses (no responses) in our experiment. The color–coding, summarized with the color–bar on the right of the plot, visualizes the response rates.

collected together. The black lines in the above figure indicate *non–target* responses which resulted the same ERP shapes. The color lines represent $P300$ responses which remained enhanced even after 500 ms mark when the next stimulus started.

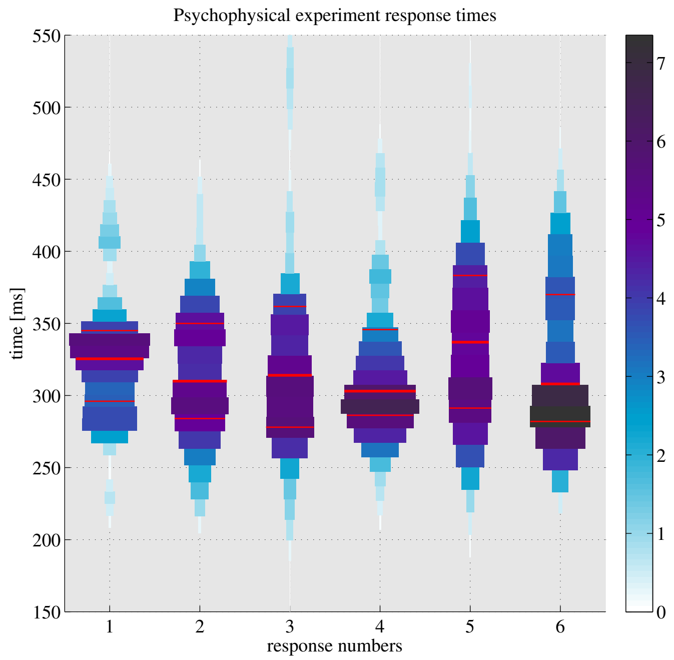


Fig. 7. Distribution boxplots depicting all the participating subjects' psychophysical experiment #1 response times. The red lines in each plot depict the $25^{th}$, $50^{th}$, and $75^{th}$ percentiles. No significant differences were observed among the medians as tested with the pairwise Wilcoxon rank sum tests. The color–coding, summarized with a color–bar on the right of the plot, visualizes the response numbers.

The results comparison of the three online BCI EEG experiments classification accuracies are presented in Figure 14. The majority of the averaged classification accuracies resulted above chance levels of 16.66%. The red bars in Figure 14 show results of the experiment #1, while the blue bars depict results of the experiment #2, and the green bars represent results of the experiment #3. The classification accuracies of the new proposed stimulus patterns (experiments #2 and #3) were not significantly improved comparing with the previously proposed approach in the experiment #1, but we could show improvements between patterns #2 and #3. We conducted pairwise t–test analyses using classification accuracies. As results, we obtained the border of significance results with $p < 0.06$ between the patterns #2 and #3, which supported the initial research hypothesis of the new patterns search.

## IV. Conclusions

This case study demonstrated results obtained with a comparison of three six–commands tactile and bone–conduction auditory approaches to BCI paradigms improvements. The experiment results obtained in this study confirmed the initial research hypothesis and stimulation patterns optimization could lead to the final BCI accuracy improvements.

The EEG experiment with the paradigm has confirmed that tactile and bone–conduction BCI paradigm can be used easily improved for online case using SWLDA classifier.

The results presented offer a step forward in the development of novel neurotechnology application. The current

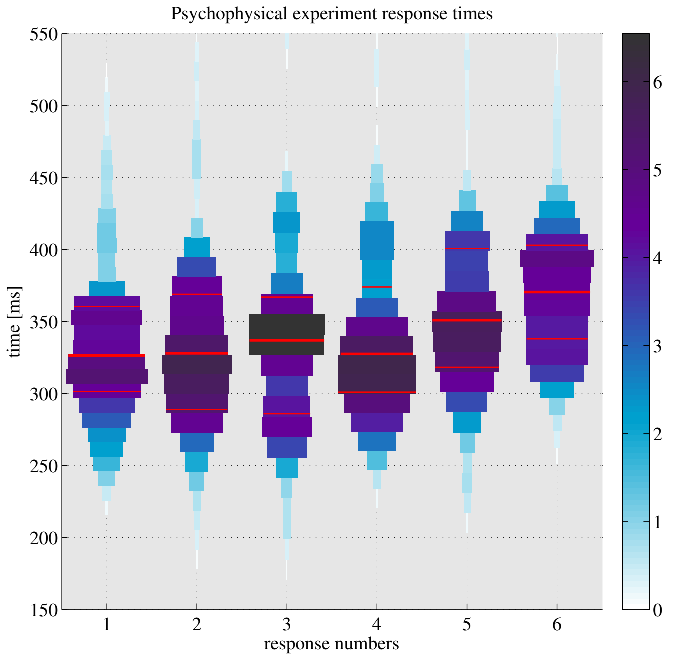


Fig. 8. Distribution boxplots depicting all the participating subjects' psychophysical experiment #2 response times. The red lines in each plot depict the $25^{th}$, $50^{th}$, and $75^{th}$ percentiles. No significant differences were observed among the medians as tested with the pairwise Wilcoxon rank sum tests. The color–coding, summarized with a color–bar on the right of the plot, visualizes the response numbers.

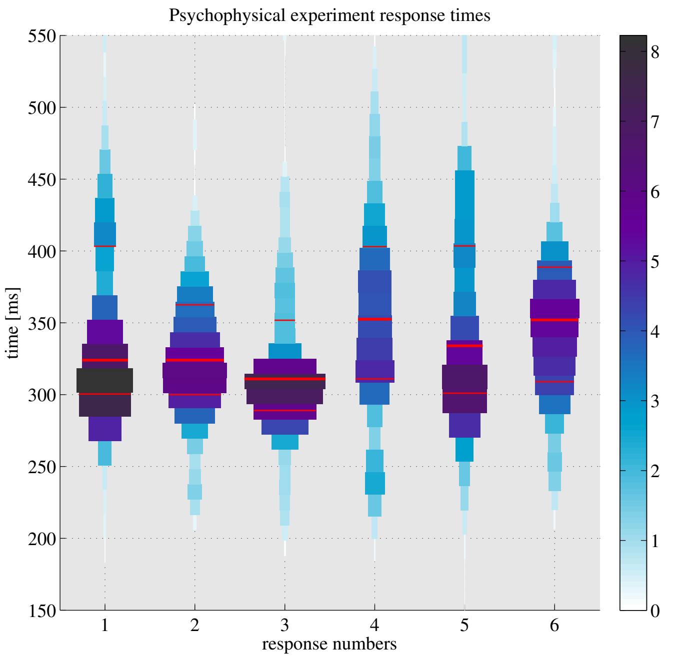


Fig. 9. Distribution boxplots depicting all the participating subjects' psychophysical experiment #3 response times. The red lines in each plot depict the $25^{th}$, $50^{th}$, and $75^{th}$ percentiles. No significant differences were observed among the medians as tested with the pairwise Wilcoxon rank sum tests. The color–coding, summarized with a color–bar on the right of the plot, visualizes the response numbers.

paradigm obviously needs still improvements and further optimizations to implement online successfully. These needs determine the major lines of study for future research.

We plan to continue this line of the tactile and bone–conduction auditory BCI research in order to further optimize stimulus patterns design.

## Acknowledgments

We would like to express our gratitude to Yoshihiro Matsumoto, the BCI-lab-group and the Multimedia Laboratory alumnus, who supported the project in the early stages with programming of BCI2000 updates.

This research was supported in part by the Strategic Information and Communications R&D Promotion Programme no. 121803027 of The Ministry of Internal Affairs and Communication in Japan, and by KAKENHI, the Japan Society for the Promotion of Science grant no. 24243062.

## References

[1] J. Wolpaw and E. W. Wolpaw, Eds., *Brain-Computer Interfaces: Principles and Practice*. Oxford University Press, 2012.

[2] T. M. Rutkowski, A. Cichocki, and D. P. Mandic, "Spatial auditory paradigms for brain computer/machine interfacing," in *International Workshop On The Principles and Applications of Spatial Hearing 2009 (IWPASH 2009) - Proceedings of the International Workshop*, Miyagi-Zao Royal Hotel, Sendai, Japan, November 11-13, 2009, p. P5.

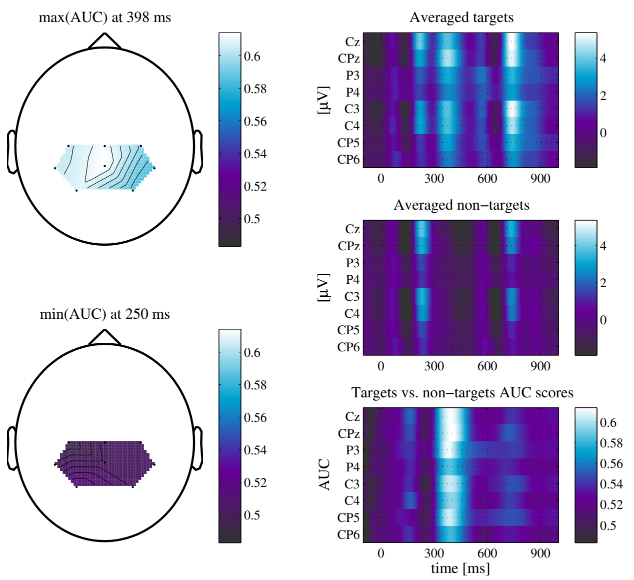


Fig. 10. All the six subjects grand mean averaged results of the EEG experiment#1. The left two panels present the head topographic plot of the *target versus non–target* area under the curve (AUC), a measure commonly used in machine learning intra–class discriminative analysis. (AUC $>$ 0.5 is usually assumed to be confirmation of feature separability).The right three panels present the averaged ERPs (six subjects; three experimental runs each with six targets repeated ten times) for *target* in the top panel; *non–target* in the middle; and *target versus non–target* AUC at the bottom.

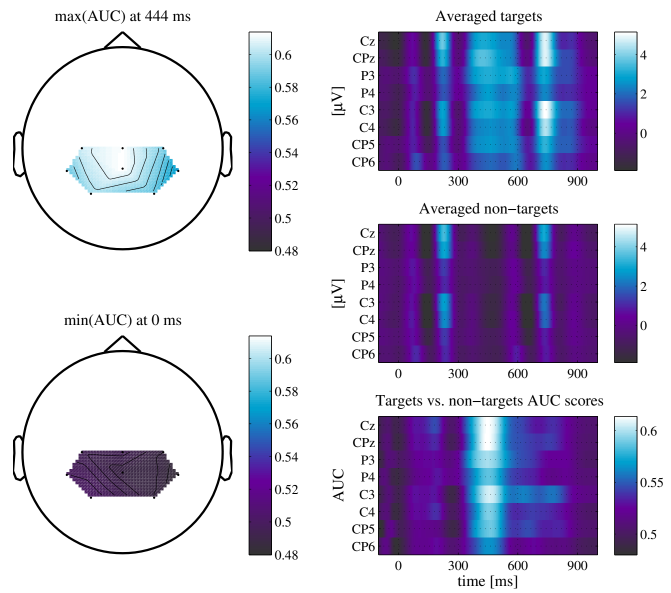


Fig. 11. All the six subjects grand mean averaged results of the EEG experiment#2. The left two panels present the head topographic plot of the *target versus non–target* area under the curve (AUC), a measure commonly used in machine learning intra–class discriminative analysis. (AUC > 0.5 is usually assumed to be confirmation of feature separability).The right three panels present the averaged ERPs (six subjects; three experimental runs each with six targets repeated ten times) for *target* in the top panel; *non–target* in the middle; and *target versus non–target* AUC at the bottom.

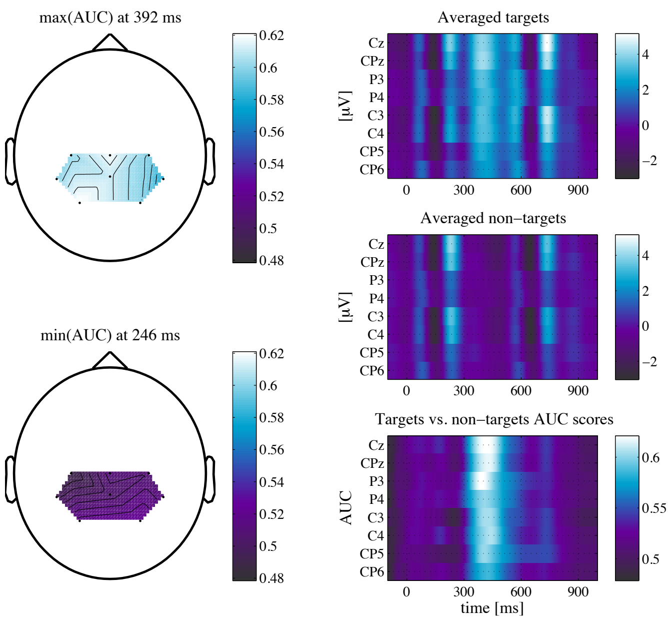


Fig. 12. All the six subjects grand mean averaged results of the EEG experiment#3. The left two panels present the head topographic plot of the *target versus non–target* area under the curve (AUC), a measure commonly used in machine learning intra–class discriminative analysis. (AUC > 0.5 is usually assumed to be confirmation of feature separability).The right three panels present the averaged ERPs (six subjects; three experimental runs each with six targets repeated ten times) for *target* in the top panel; *non–target* in the middle; and *target versus non–target* AUC at the bottom.

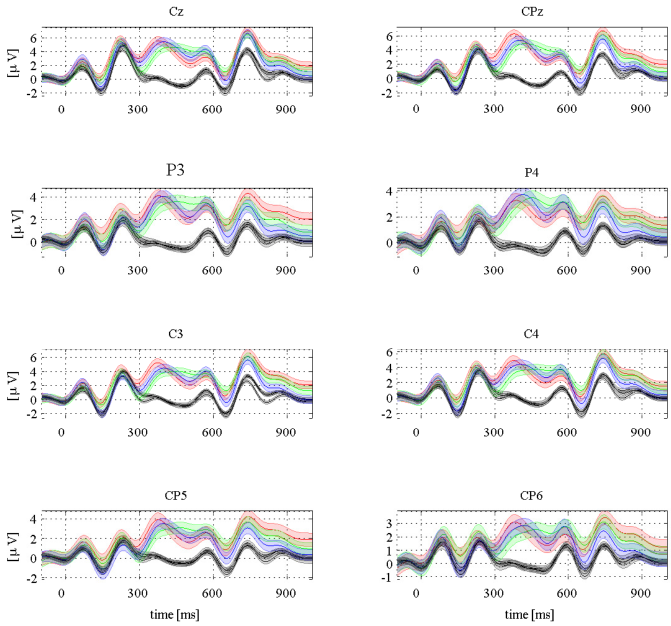


Fig. 13. ERP to real and virtual sound image stimuli for all EEG electrodes used in the experiments conducted. The red lines represent the grand mean averaged *target* responses to the EEG experiment#1, while the green lines indicate *target* responses to the EEG experiment#2, and the blue lines show *target* response to the EEG experiment#3, remaining black lines mean *non–target* response to the all of EEG experiment, respectively. Error bars depicting standard errors are also drawn around each of the averaged responses.


[3] G. Muller-Putz, R. Scherer, C. Neuper, and G. Pfurtscheller, "Steady-state somatosensory evoked potentials: suitable brain signals for brain-computer interfaces?" *Neural Systems and Rehabilitation Engineering, IEEE Transactions on*, vol. 14, no. 1, pp. 30–37, March 2006.


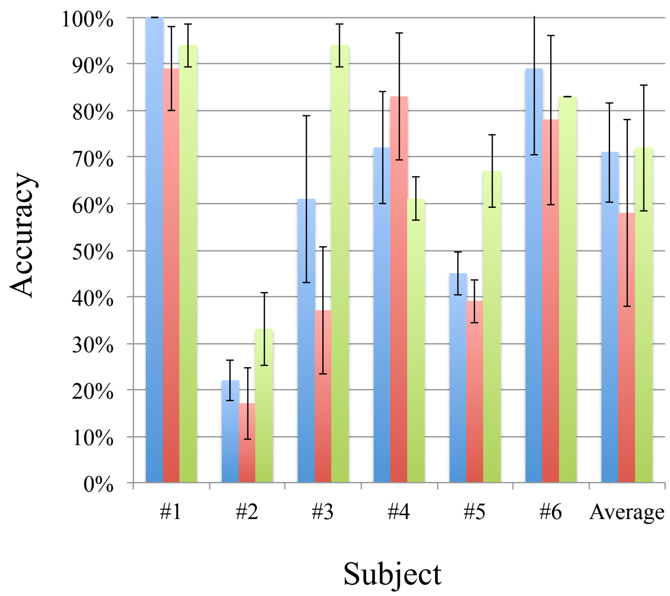


Fig. 14. The accuracy results comparing of the three experiments with various stimulus patterns. Blue, red and green bars stand for experiments #1, #2 and #3 respectively. The horizontal axis represents the subject numbers and the vertical one the accuracy rates in percents. Error bars depict standard errors.

[4] A.-M. Brouwer and J. B. F. Van Erp, "A tactile P300 brain-computer interface," *Frontiers in Neuroscience*, vol. 4, no. 19, 2010. [Online]. Available: http://www.frontiersin.org/neuroprosthetics/10.3389/fnins.2010.00019/abstract

[5] M. van der Waal, M. Severens, J. Geuze, and P. Desain, "Introducing the tactile speller: an ERP-based brain–computer interface for communication," *Journal of Neural Engineering*, vol. 9, no. 4, p. 045002, 2012. [Online]. Available: http://stacks.iop.org/1741-2552/9/i=4/a=045002

[6] H. Mori, Y. Matsumoto, V. Kryssanov, E. Cooper, H. Ogawa, S. Makino, Z. Struzik, and T. M. Rutkowski, "Multi-command tactile brain computer interface: A feasibility study," in *Haptic and Audio Interaction Design 2013 (HAID 2013)*, ser. Lecture Notes in Computer Science, I. Oakley and S. Brewster, Eds. Springer Verlag Berlin Heidelberg, 2013, vol. 7989, pp. 50–59. [Online]. Available: http://arxiv.org/abs/1305.4319

[7] T. Kaufmann, E. M. Holz, and A. Kuebler, "Comparison of tactile, auditory and visual modality for brain-computer interface use: A case study with a patient in the locked-in state," *Frontiers in Neuroscience*, vol. 7, no. 129, 2013. [Online]. Available: http://www.frontiersin.org/neuroprosthetics/10.3389/fnins.2013.00129/abstract

[8] H. Mori, Y. Matsumoto, Z. R. Struzik, K. Mori, S. Makino, D. Mandic, and T. M. Rutkowski, "Multi-command tactile and auditory brain computer interface based on head position stimulation," in *Proceedings of the Fifth International Brain-Computer Interface Meeting 2013*. Asilomar Conference Center, Pacific Grove, CA USA: Graz University of Technology Publishing House, Austria, June 3-7, 2013, p. Article ID: 095. [Online]. Available: http://castor.tugraz.at/doku/BCIMeeting2013/095.pdf

[9] T. M. Rutkowski and H. Mori, "Tactile and bone–conduction auditory brain computer interface for vision and hearing impaired users," *Journal of Neuroscience Methods*, p. Available online 21 April 2014, 2014. [Online]. Available: http://dx.doi.org/10.1016/j.jneumeth.2014.04.010

[10] V. Jurcak, D. Tsuzuki, and I. Dan, "10/20, 10/10, and 10/5 systems revisited: Their validity as relative head-surface-based positioning systems," *NeuroImage*, vol. 34, no. 4, pp. 1600 – 1611, 2007. [Online]. Available: http://www.sciencedirect.com/science/article/pii/S1053811906009724

[11] G. Schalk and J. Mellinger, *A Practical Guide to Brain–Computer Interfacing with BCI2000*. Springer-Verlag London Limited, 2010.

[12] Y. Matsumoto, S. Makino, K. Mori, and T. M. Rutkowski, "Classifying p300 responses to vowel stimuli for auditory brain-computer interface," in *Signal and Information Processing Association Annual Summit and Conference (APSIPA), 2013 Asia-Pacific*, 2013, pp. 1–5, paper ID 388. [Online]. Available: http://www.apsipa.org/proceedings_2013/papers/388_Classifying-P300-Matsumoto-2933943.pdf

[13] Y. Matsumoto, "Application of stimulus-based ensemble classifier to spatial auditory BCI speller," Master Thesis, Graduate School of Systems and Information Engineering - University of Tsukuba, Tsukuba, Japan, January 2014.

[14] D. J. Krusienski, E. W. Sellers, F. Cabestaing, S. Bayoudh, D. J. McFarland, T. M. Vaughan, and J. R. Wolpaw, "A comparison of classification techniques for the P300 speller," *Journal of Neural Engineering*, vol. 3, no. 4, p. 299, 2006. [Online]. Available: http://stacks.iop.org/1741-2552/3/i=4/a=007